RP Current Trends In Applied Sciences
Vol. 1, No. 1 (October – December 2022) pp. 11–15
e-ISSN: 2583-7486

RESEARCH PLATEAU PUBLISHERS

Cite this article: Sanjay, Nonlinear scattering of coherent optical pulses in a medium containing randomly distributed quantum dots, *RP Cur. Tr. Appl. Sci.* **1** (2022) 11–15.

Original Research Article

Nonlinear scattering of coherent optical pulses in a medium containing randomly distributed quantum dots

Jaivir Singh
Department of Physics, Janta Vidya Mandir Ganpat Rai Rasiwasia College, Charkhi Dadri – 127306, Haryana, India
*Corresponding author, E-mail: jaivir.bmu@gmail.com

ARTICLE HISTORY
Received: 19 Sept. 2022
Revised: 04 Nov. 2022
Accepted: 06 Nov. 2022
Published online: 10 Nov. 2022

KEYWORDS
Quantum dot GaAs/GaAlAs;
Excitonic resonance;
Nonlinear scattering;
Optical properties.

ABSTRACT
In this research, a straightforward model for calculating the optical characteristics of a medium containing randomly distributed QDs is proposed. For the purpose of obtaining analytical results, some simplifications, such as the presumption of limitless walls and huge hole masses, have been made. When compared to earlier methods, where the dots were considered like points and the scattering effects were ignored, the simplified model is still an improvement. The method was used to construct an effective energy- and size-dependent complex dielectric function for a single GaAs/GaAlAs QD while accounting for coherence effects on the amplitude of the dipole densities and excitonic transitions. Coherence effects can be seen in the lineshapes of the peaks in the fictitious portion of the susceptibility and the oscillator strengths. It has been discovered that as the QD's radius is reduced, the excitonic energies and oscillator strengths rise. The dispersed pulse exhibits an angular dependence for parallel and perpendicular polarisation to the reference plane that is equal close and distant from the resonances, with the intensity being significantly higher in the former case.

1. Introduction

Excitonic transitions can be used to explain the optical properties of quantum dots (QDs). Excitonic effects are strengthened as a result of the internment of quasi-particles in a dot, which enhances the oscillator strength and binding energy of excitons density [1-3]. Calculations of oscillator strengths and excitonic binding energies have taken a lot of time.

Utilising the sphere-shaped model of QDs, the author's goal is to go into great depth about how exciton resonance affect the characteristics of dispersed pulse. Making the use of the necessary Green functions, the author solves the constitutive equations using the Stahl real density matrix (RDM) technique. The author determined the polarisation and effective (isotropic) dielectric susceptibility function of the quantum dot using the coherent amplitudes. Using this technique, one can account for the electromagnetic wave's and carriers' coherence within the QD. Additionally, the contribution of the continuum states is accurately described. The author derived the scattered pulse amplitudes from the effective QD susceptibility using the classical theory of Mie resonances. The author then go into its characteristics in relation to important physical factors including the scattering angle, incident pulse frequency, and dot radius. For GaAs/$Ga_{1-x}Al_xAs$ QDs, numerical results are provided and analysed.

2. Theoretical formulations

According to Stahl's method, the optical characteristics of a multi - band semiconductors at the fundamental gap in the weaker field regime are described by a collection of governing equations on the bandgap transformation amplitudes $Y_{\lambda\mu}(\vec{r}_e,\vec{r}_h)$ of the *e-h* pair of coordinates, r_e and r_h, respectively [4-7] as:

$$\partial_t Y_{\lambda\mu} + \frac{i}{\hbar} H_{\lambda\mu} Y_{\lambda\mu} = \frac{i}{\hbar}[\vec{M}_{\lambda\mu}\vec{E} - \Gamma_{\lambda\mu} Y_{\lambda\mu}], \quad (1)$$

where $H_{\lambda\mu}$ represents the two-band effective mass Hamiltonian, together with *e-h* interaction; $\vec{E}$ represents the laser pulse electric field, $\Gamma_{\lambda\mu}$ stands for the phenomenological damping coefficient, and $M_{\lambda\mu}$ represent the coupling functions defined as the transitional dipole moment densities, which may be expressed in the following manner [6]:

$$M_{\lambda\mu}(\vec{r}_e,\vec{r}_h) = \vec{M}_{0\lambda\mu} D_{\lambda\mu}(\vec{r}_e - \vec{r}_h), \quad (2)$$

$M_{\lambda\mu}$ is the equivalent integrated strength, whose explicit expression is provided in Ref. [6], and

$$D_{\lambda\mu}(\vec{r}_e - \vec{r}_h) = \frac{1}{(4\pi)^{1/2} r r_{0\lambda\mu}^2} \exp\left(-\frac{r}{r_{0\lambda\mu}}\right), \quad (3)$$

the so-called coherence radius, with $r_{0\lambda\mu}$ being the transition dipole density. The author found this is useful to take the coherent radius as independent constant and to assume that they have values in the range of 0.1 to 0.3 of the exciton Bohr's radius, as in the majority of Stahl method uses.

We may determine the polarisation within the quantum dot from the coherent amplitudes of Eqs. (1) and (2).

$$P(\vec{r}_{CM}) = 2\sum_{\lambda\mu} \vec{M}_{\lambda\mu} \int Y_{\lambda\mu}(\vec{r},\vec{r}_{CM}) D_{\lambda\mu}(\vec{r}) d^3\vec{r}. \quad (4)$$

In Eq. (4), $\vec{r} = \vec{r}_e - \vec{r}_h$ stand for the relative coordinate and $\vec{r}_{CM}$ represents center of mass (CM) of the system.

To ascertain the optical characteristics of a matrix comprising QDs, one must simultaneously solve the fundamental Eqs. (1), Maxwell's equations out beyond and within the QD, where the excitonic polarisation is determined by Eq. (4), and applies boundary constraints. The author notice that the interpretation of the $P(\vec{r}_{CM})$ in Maxwell's equation relates the excitonic CM coordinates inside the QD, but in the present analysis, the fundamental equations refer to a 6-D configurationally space $(\vec{r}_e, \vec{r}_h)$, where the author assumed adequate boundary conditions for *e-h* motion. The present problem is very challenging because of this intricacy, but with the help of the following simplifying assumptions, one can find analytical answers. In order to force the proper normalisation of Eq, the author supposed that both electrons and holes have unlimited confinement potentials (2). To allow for the disregard of the corresponding kinetic term in the Hamiltonian $H_{\lambda\mu}$, it is assumed that the effective mass of the holes is significantly more than the mass of the electron [8]. By using the proper gap energies $E_{gn_hl_hH}$, $E_{gn_hl_hL}$, one can account for how the heavy and light holes' varied masses affect the confinement on them. Label the hole states here with n_h and l_h.

The aforementioned assumptions and the placement of the hole at the center of QD, which simplifies computation and results in theoretical calculations for the QD susceptibility, have no bearing on the primary physical subject under investigation, the scattering of an electromagnetic pulse by an ensemble of QDs.

The author employed a dielectric screened Coulomb interaction among *e-h* pairs and the effective mass approximation for the valence and the conduction bands, separating heavy- and light -band effective masses. Using the necessary Green functions, the author solved the constitutive Eqs. (1), determine the polarisation, and then calculate the QD susceptibility [9].

$$\chi_{ex} = \sum_{\lambda=H,L} \frac{2}{\varepsilon_0}\left(\frac{2m_e}{\hbar^2}\frac{1}{a_e^*}\right) \times \sum_{n_hl_hl_m} M_{0lm\lambda}^2 \int_0^{R/a_e^*}\int_0^{R/a_e^*} \rho^2 d\rho\rho'^2 D_{lm\lambda}(\rho) g_{n_hl_hm\lambda}(\rho,\rho') D_{lm\lambda}(\rho') , \quad (5)$$

where

$$g_{nn_hl_hm\lambda}(\rho,\rho') = C(4\kappa^2\rho,\rho')^l \exp[-\kappa(\rho+\rho')M(a_l,b_l,2\kappa\rho^<) \times[U(a_l,b_l,2\kappa\rho^<) + A_lM(a_l,b_l,2\kappa\rho^<)] , \quad (6)$$

$$\kappa^2_{n_hl_hm\lambda} = \frac{2m_e}{\hbar^2}(E_{gn_hl_h\lambda} - \hbar\omega - i\Gamma_\lambda) ,$$

$$C = \frac{2\kappa\Gamma(a_l)}{\Gamma(b_l)} ,$$

$$A_l = -\frac{U(a_l,b_l,2\kappa R/a_e^*)}{M(a_l,b_l,2\kappa R/a_e^*)} ,$$

$a_l = l + 1 - \frac{1}{\kappa}$, and $b_l = 2l + 2$.

Kummer's first-type and second-type functions are $M(a,b,z)$ and $U(a,b,z)$, respectively [10]. The author noted that only the term $l = 0$ contributes to the susceptibility after selecting an isotropic expression for the dipole density (2).

Using the parameters acceptable for GaAs in an AlAs matrix and the approximation of infinite barriers, the author has performed thorough computations for QD of various radii. Figure 1 reports the findings for the actual and fictitious components of the QD's susceptibility. One can see that resonances correspond to the excitonic transitions in the imaginary part of χ_{ex}. The author also showed in Figure 2 how the radius of the QD affects both the binding energy and the lowest exciton transition. While the bulk value already exists for QD having dimensions of approximately five times the Bohr radii, one may observe that an influence of confinement predominates over the rise in binding energy for tiny radii relative to Bohr radii.

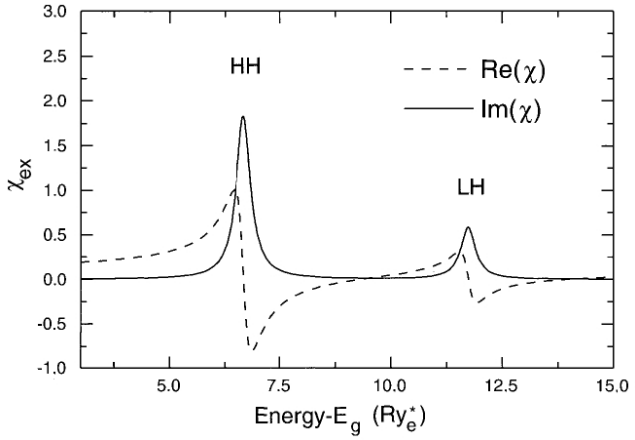

Figure 1. Variation of real and imaginary parts of χ versus E_g for $GaAs/Ga_{1-x}Al_xAs$ QD of dimensions $R = 1a_e^*$.

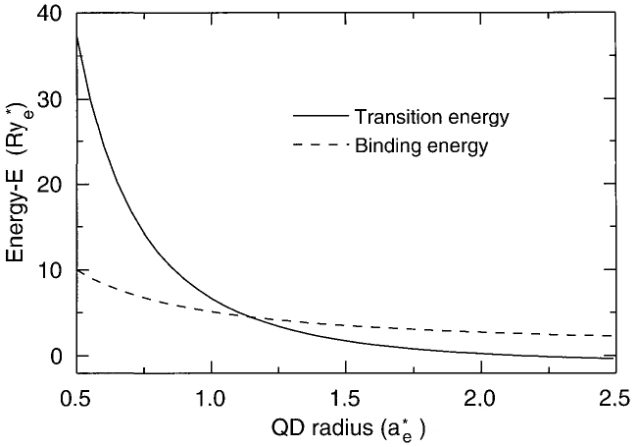

Figure 2. Energy of the lowest optical transition and binding energy of the excitons as functions of the dot radius.

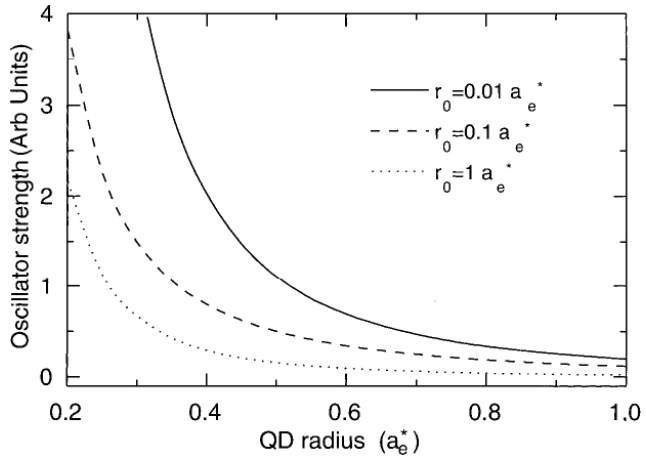

Figure 3. Variation of the lowest exciton transition oscillator strength with QD radius.

The oscillator strength of optical transition density likewise rises as a result of confinement. For various values of the coherence radii, the author reported in Figure 3 the estimated magnitudes of the oscillator strength density versus QD radius. Decreasing oscillator strength and resonant peak heights are the results of rising coherence radius.

3. Results and discussion

Let us now go through how a QD of radius R that is submerged in the isotropic and homogeneous media reacts optically to an incident linearly polarised electromagnetic pulse $(E_x^{(i)},0,0)$,

$$E_x^{(i)} = E^i \exp(ik^{(I)}z), \tag{7}$$

where the superscript *I* denotes the quantities that apply to the area around the dot. The author employed the equation applicable to a spherical dot with a mean homogenous susceptibility for wave vector $k^{(II)}$ inside the QD.

$$\frac{c^2k^{(II)2}}{\omega^2} = \varepsilon_b + \chi_{ex}, \tag{8}$$

where ε_b stands for dielectric function at the frequency greater than the resonant frequency. An electromagnetic pulse will be generated inside QD by the coherent pulse; as a result another pulse $\vec{E}^{(s)}$ will be scattered outside the dot. The QD's modest size in relation to the wavelength we've been thinking about is what drives this approximation.

The author used the classic theory as developed by Mie and Debye [11, 12] to determine the amplitudes of scattered coherent pulse in the frequency domain in which LH and HH excitonic states are significant, considering the circumstances of GaAs/$Ga_{1-x}Al_xAs$ or $Ga_xIn_{1-x}As$/GaAs QDs. After calculating the effective QD susceptibility χ_{ex} and, consequently, the effective dielectric function $\varepsilon^{(II)}$.

The extinction cross-section of a QD is calculated from them in terms of the QD radius and the input pulse energy, appearing through the parameter

$$q = \hbar\omega(\varepsilon^{(I)})^{1/2}\frac{R}{\hbar c}. \tag{9}$$

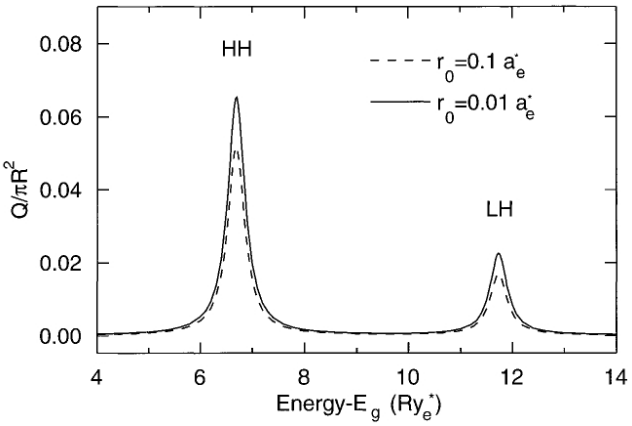

Figure 4. For energies close to the lowest excitonic states, the cross-section Q of QD with $R = 1a_e^*$. The two curves show how coherence has an impact on line forms and correspond to various coherence radius values.

The rate of energy loss, which includes both dissipation and scattering, to the rate of incoming flux is known as the extinction cross-section Q. Figure 4 shows the findings for the cross-section of a QD with radius a_e^* produced in Table 1 parameters. One can see that the cross-section Q is essentially nonexistent away from the resonances because the ratio $q = 2\pi R/\lambda$ in this case is so small (~ 0:1). Additionally, one can see that it grows as energy rises (because it decreases), with twice the geometric cross-section serving as its upper limit $\lambda \to 0$. However, very strong peaks that correlate to the QD's excitonic resonances may be seen in the cross-section. Ruppin [13] has studied this issue in relation to the fundamental scattering of QD with the effective dielectric function.

Table 1. Parameters that apply to bulk GaAs (masses in m_0, energy in meV, and length in angstrom)

Parameter	Value
m_e	0.0665
m_{hH}	0.34
m_{hL}	0.094
ε_b(GaAs)	12.53
ε_b(AlAs)	10.03
$\left\|\vec{P}_H(0)\right\|^2/(2m_0)$	5.75
$\left\|\vec{P}_L(0)\right\|^2/(2m_0)$	1.92
Ry_e^*	5.76
a_e^*	99.6
$E_{gH} = E_{gL}$	1519.1
$r_{0H} = r_{0L}$	$0.1a_e^*$
$\Gamma_H = \Gamma_L$	$0.2\mathrm{Ry}_e^*$

Finally, let us look at the scattered wave's polarisation and strength. The author calculates the square value of electric field's amplitude and take into account polarisation perpendicular ($\perp$) and parallel ($\|$) to the plane of observation, described via set of angle coordinates (θ,ϕ) of scattered pulse,

ϕ representing the angle with the incoming electric field's polarisation direction and θ the angle with respect to the incident pulse propagation direction (z). The author arrived at the following formulas by taking into account the approximation of huge distance $r >> \lambda$:

$$\left|E_{\theta}^{(s)}\right|^2 = I_{\parallel}^{(s)} \cos^2\phi\,, \tag{10a}$$

$$\left|E_{\phi}^{(s)}\right|^2 = I_{\perp}^{(s)} \sin^2\phi\,, \tag{10b}$$

where

$$I_{\parallel}^{(s)} = \frac{\lambda^{(I)2}}{4\pi^2 r^2}\left|\sum_{l=1}^{\infty}(-1)^l\left({}^{e}B_l P^{(1)'}(\cos\theta)\sin\theta - {}^{m}B_l \frac{P_l^{(1)}(\cos\theta)}{\sin\theta}\right)\right|^2, \tag{11a}$$

$$I_{\perp}^{(s)} = \frac{\lambda^{(I)2}}{4\pi^2 r^2}\left|\sum_{l=1}^{\infty}(-1)^l\left({}^{e}B_l \frac{P^{(1)}(\cos\theta)}{\sin\theta} - {}^{m}B_l P_l^{(1)'}(\cos\theta)\sin\theta\right)\right|^2, \tag{11b}$$

where ${}^{e}B_l$, ${}^{m}B_l$ are the Mie coefficients [11, 12], $E_{\theta}^{(s)}$, $E_{\phi}^{(s)}$ stand for components of electric field of scattered pulse, and $P_l^{(1)}$ are associated Legendre polynomials.

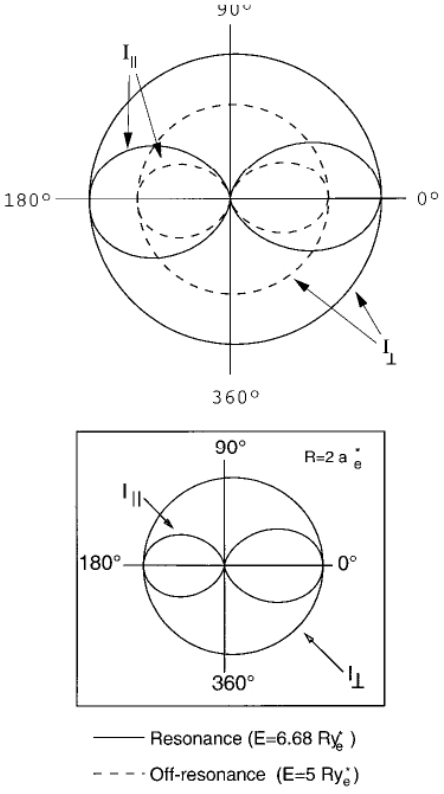

Figure 5. Linearly polarised light scattering polar diagrams.

The author determined the intensity and polarisation of dispersed signal in terms of the observation angle θ and for two frequencies that were selected to be far and close to an excitonic resonance, respectively. Figure 5 displays these polar diagrams for the QD with radius $1a_e^*$. The inner curve radii vector are dependent on intensity $I_{\parallel}^{(s)}$, while the radii vector of the out-side curves are dependent on intensity $I_{\perp}^{(s)}$. One may see the isotropy of $I_{\perp}$ and the odd angular dependency for $I_{\parallel}$. There exists a dip in the symmetry plane and an intensity peak in both the forward and backward directions for $\theta = 0^o$ and $\theta = 90^o$, respectively. As would be predicted by the criterion $\lambda >> R$, this distribution is a classic dipolar one. By increasing the QD radius, one is able to produce asymmetric polar diagrams that are comparable to those seen in the problem's literature [12]. This happens for frequencies both on and off resonance, however the scattered pulse intensities at resonance are substantially higher. Figure 6 shows the intensity of the dispersed pulse for $\theta = 0^o$ as a function of energy $\hbar\omega$ to illustrate this improvement.

4. Conclusions

In order to determine the optical characteristics of QDs, in this paper, the author built a straightforward model that specifically takes into account the interaction of an incoming coherent pulse on a QD. In order to get analytical results, the author has adopted several simplifications, such as the assumption of limitless walls and enormous hole masses. When compared to earlier methods, when the dots were considered like points and the scattering effects were ignored, our simplified model is nevertheless an improvement. In order to compute size-dependent complex dielectric function and an effective susceptibility that takes into account the transition between exciton states and includes coherence effects on the amplitude of the dipoles per unit volume, the author used the aforementioned method to a single GaAs/GaAlAs QD. Coherence effects can be seen in the lineshapes of the peaks in the fictitious portion of the susceptibility and the oscillator strengths. The author demonstrated that the oscillator strengths and excitonic energy rise as the QD's radius decreases. The dispersed pulse exhibits an angular dependency for perpendicular as well as parallel polarisation to the reference plane that is equal close and distant from the resonance, with the intensity being significantly higher in the former case. All correlation and size distribution effects have not been taken into account because impacts are only computed for a single quantum dot in the current paper. This is accurate since the author took into account a low density of uniformly spaced dots.

References

[1] U. Woggon, S.V. Gaponenko, Excitons in quantum dots, *phys. stat. sol.* (*b*) **189** (1995) 285-343.

[2] P.Y. Yu, M. Cardona, Fundamentals of Semiconductors, Springer-Verlag, Berlin (1996).

[3] U. Woggon, Optical Properties of Semiconductor Quantum Dots, Springer-Verlag, Berlin (1997).

[4] A. Stahl, I. Balslev, Electrodynamics of the Semiconductor Band Edge, Springer-Verlag, Berlin/Heidelberg/New York (1987).

[5] I. Balslev, R. Zimmermann, A. Stahl, Two-band density-matrix approach to nonlinear optics of excitons, *Phys. Rev. B* **40** (1989) 4095-4104.

[6] G. Czajkowski, F. Bassani, A. Tredicucci, Polaronic effects in superlattices, *Phys. Rev. B* **54** (1996) 2035-2043.

[7] V.M. Axt, S. Mukamel, Nonlinear optics of semiconductor and molecular nanostructures; a common prospective, *Rev. Mod. Phys*. **70** (1998) 145-174.

[8] J.H. Yuan, L.L. Wang, Z.Y. Xiong, N. Chen, Z.H. Zhang, Y.X. Zhao, Hydrogenic impurity effect on the optical nonlinear

absorption properties of a spherical quantum dots with a parabolic potential, *Eur. Phys. J. Plus* **133** (2018) 395.

[9] P. Wyborski, P. Podemski, P.A. Wronski, F. Jabeen, S. Hofling, G. Sek, Electronic and optical properties of InAs QDs grown by MBE on InGaAs metamorphic buffer, *Materials* (*Basel*) **15** (2022) 1071.

[10] I.R. Jahromi, G. Juska, S. Varo, F.B. Basset, F. Salusti, R. Trotta, A. Gocalinska, F. Mattana, E. Pelucchi, Optical properties and symmetry optimization of spectrally (excitonically) uniform site-controlled GaAs pyramidal quantum dots, *Appl. Phys. Lett*. **118** (2021) 073103.

[11] G. Mie, Gustav Mie and the scattering and absorption of light by particles, *Ann. Phys*. **25** (1908) 377-445.

[12] M. Born, E. Wolf, Principles of Optics, Pergamon Press, Oxford (1986) Chap. 13.

[13] R. Ruppin, Electromagnetic energy in dispersive spheres, *J. Opt. Soc. Am. A* **18** (1998) 524-527.